Available online at www.eccomasproceedia.org
Eccomas Proceedia COMPDYN (2023) 4511-4522

ECCOMAS
Proceedia

COMPDYN 2023
9th ECCOMAS Thematic Conference on
Computational Methods in Structural Dynamics and Earthquake Engineering
M. Papadrakakis, M. Fragiadakis (eds.)
Athens, Greece, 12-14 June 2023

FINITE ELEMENT MODELING OF SUSPENDED CEILING SYSTEMS BASED ON EXTENSIVE COMPONENT TESTING AND MODEL EVALUATION VIA SHAKING TABLE TESTS: POP RIVET AND SEISMIC CLIP PERIMETER CONNECTIONS

Shakhzod M. Takhirov[1] **and Yelena Straight**[2]

[1] Dept. of Civil and Environmental Engineering, University of California, Berkeley,
337 Davis Hall, Berkeley, California, 94720, USA
e-mail: takhirov@berkeley.edu

[2] Building Codes and Standards Manager, USG Corporation
550 West Adams Street, Chicago, IL 60661, USA
e-mail: YStraight@usg.com

Abstract

This paper is focused on a finite element (FE) modeling of suspended ceiling systems. It is well-known that for installation in regions with high seismic activity, these non-structural systems need to pass seismic evaluation tests on a shaking table. Using a shaking table can be expensive, especially when developing new components and systems might require a few iterations. The goal of this modeling paper is to develop an approach that can be used as a cost-effective alternative for the development of new components and systems. A numerical model can predict the performance of the newly developed system, identify its weak links (if any), and help to develop solutions that address any shortcomings. This paper presents an approach based on developing a FE model, the performance of which closely correlates to that of the actual system. It is based on a series of component tests that are less expensive than shaking table testing. The results of the component testing are used in modeling components of the FE model. The evaluation of the model's performance at the system level is conducted by comparing its performance to that of the actual system in a seismic evaluation test via shaking table testing. The actual system was extensively instrumented for the shaking table tests. The instrumentation included position transducers, accelerometers, and strain gages. This paper discussed this approach in detail and summarized the results of the experimental and numerical studies.

Keywords: Non-structural Components, Suspended Ceiling Systems, Component Testing, Shaking Table Testing, Finite Element Modeling, Seismic Evaluation.

ISSN:2623-3347
Peer-review under responsibility of the organizing committee of COMPDYN 2023.
doi: 10.7712/120123.10737.21317

1 INTRODUCTION

This paper is focused on suspended ceiling systems built with the USG's DX components. A pop riveted connection was selected for the fixed sides and a seismic clip was chosen for the perimeter connections of the floating sides. The extensive experimental program focused both on component testing of the system and on shaking table tests of the system constructed from these components. Based on the results of the component testing program, a finite element model was generated. The model's seismic performance was compared to the results of the shaking table tests.

2 COMPONENT TESTING

Failures of suspended ceiling systems usually occur at the connection points. This section of the paper is focused on component testing of the major connections of the suspended ceiling system. For the suspended ceiling studied in this paper, the following connections were studied in component testing. First, a main tee or a cross tee to the perimeter molding on the fixed sides was evaluated in quasi-static cyclic loading. Second, a cross tee to a cross tee connection was tested in quasi-static cyclic loading. Third, a main tee to a main tee connection was also evaluated during this experimental program. The latter two connection tests are referenced as joint tests in this paper.

2.1 Experimental Setups for Component Testing

The purpose of all component tests was to evaluate the overall performance of each connection along with its ultimate capacity. At least three tests per connection were conducted. The test samples were randomly selected. A list of tests is provided in Table 1. The conducted tests were part of a multiyear extensive program with the results summarized in the technical test reports [1-2].

Connection	MT/CT name	Specimen name	Note	Reference
MT to M7 via PR	DX24	USG2015-Sp01	Perimeter at fixed side	[1]
CT to M7 via PR	DX424	USG2015-Sp03	Perimeter at fixed side	[1]
CT to M7 via PR	DX424	USG2015-Sp04	Perimeter at fixed side	[1]
CT to M7 via PR	DX424	USG2015-Sp10	Perimeter at fixed side	[1]
MT to MT joint	DX26 to DX26	USG2021-Sp47	Joint	[2]
CT to CT joint	DX424 to DX424	USG2021-Sp44	Joint	[2]
CT to CT joint	DX424 to DX424	USG2021-Sp45	Joint	[2]
CT to CT joint	DX424 to DX424	USG2021-Sp48	Joint	[2]
CT to CT joint	DX424 to DX216	USG2021-Sp40	Joint	[2]
CT to CT joint	DX424 to DX216	USG2021-Sp41	Joint	[2]
CT to CT joint	DX424 to DX216	USG2021-Sp50	Joint	[2]
CT to CT joint	DX216 to DX216	USG2021-Sp35	Joint	[2]
CT to CT joint	DX216 to DX216	USG2021-Sp37	Joint	[2]
CT to CT joint	DX216 to DX216	USG2021-Sp38	Joint	[2]

Table 1: Summary of the component tests (all connections were tested in cyclic loading except USG2015-Sp01).

In Table 1 MT stands for a main tee, CT stands for a cross tee, and PR stands for a pop rivet. These abbreviations will be used herein. In addition, the following USG components are listed in Table 1: M7 is USG's wall molding, DX24 and DX26 are USG's main tees, DX424 and DX216 are USG's cross tees.

The connections were tested in two major configurations. The first configuration was developed for testing perimeter connections as presented in Figure 1. As shown in Figure 1a, the experimental setup consisted of an actuator applying the load to one side of the connection, with a reaction frame attached to the opposite side of the connection. In the case of the perimeter connection, the reaction frame was installed at 90 degrees to the axis of loading whereas for the joint connection, the loading and the reacting sides were in-line with the actuator. To ensure that the force is always applied along the same axis, the actuator was guided by a linear bearing system as presented in Figure 1b. The second configuration was developed for testing joints as presented in Figure 2.

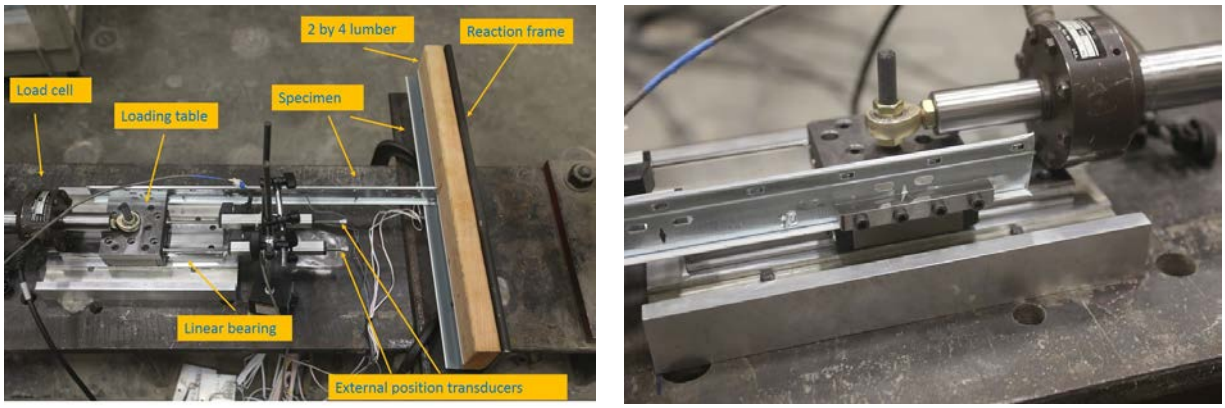

a) Major components b) Actuator guided by a linear bearing system

Figure 1: Experimental setup for component testing of perimeter connections.

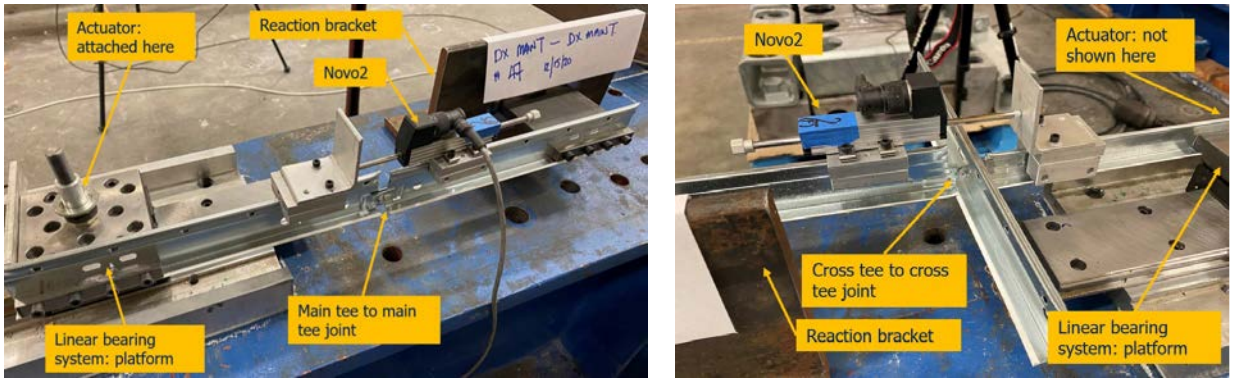

a) MT to MT b) CT to CT with MT at 90 degrees

Figure 2: Experimental setup for component testing of joints.

2.2 Tested Configurations and Test Results

Almost all component tests were conducted by imposing a cyclic loading as presented in Figure 3a. The test protocol consisted of groups of three cycles at the same amplitude, which were then incrementally increased. The response of the test specimens was monitored by a few position transducers as presented in Figure 1 and Figure 2. In addition, a tri-axial strain gage was installed at the wall molding, adjacent to the pop rivet, as presented in Figure 3b.

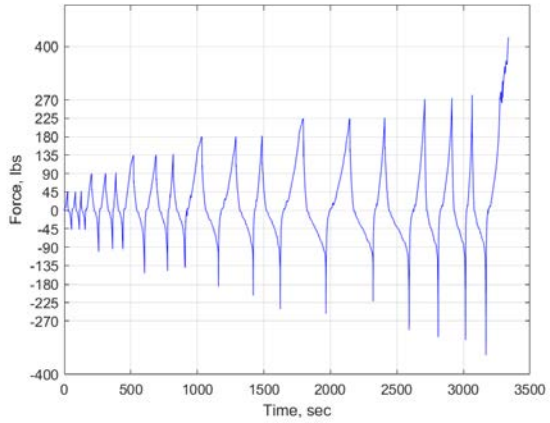

a) Typical loading protocol (1 lb = 4.4 N)

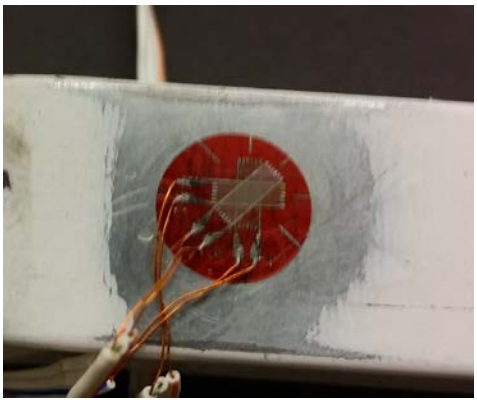

b) Tri-axial strain gage installed adjacent to the pop rivet location

Figure 3: Test protocol and additional instrumentation.

Typical test results are presented in Figure 4a. In this case a cyclic performance of USG2015-Sp10 (noted as Sp10 in the plot) is compared to a monotonic pull test conducted on USG2015-Sp01 (noted as Sp01 in the plot). The failure of the connection is related to the tear failure of the hole in the cross tee as shown in Figure 4b. As can be seen from Figure 4a a main tee in monotonic testing has a larger capacity than the cross tee in cyclic loading. This result can be explained by the fact that the flange of the main tee is thicker than that of the cross tee. In addition, it was evident that an ultra-low cycle loading fatigue affects the capacity of the cross tee in a significant way.

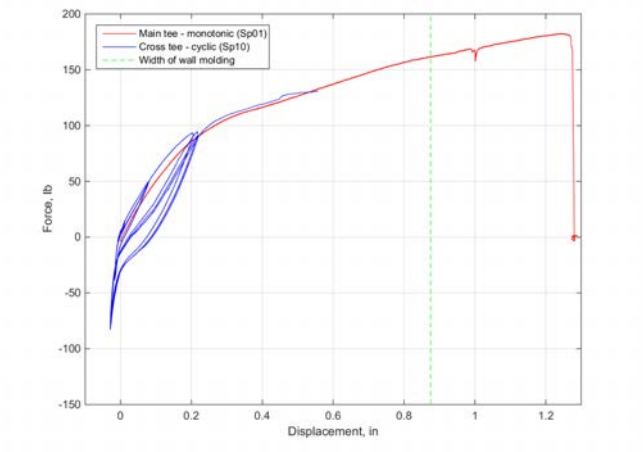

a) Typical test result (1 lb = 4.4 N; 1 in = 25.4 mm)

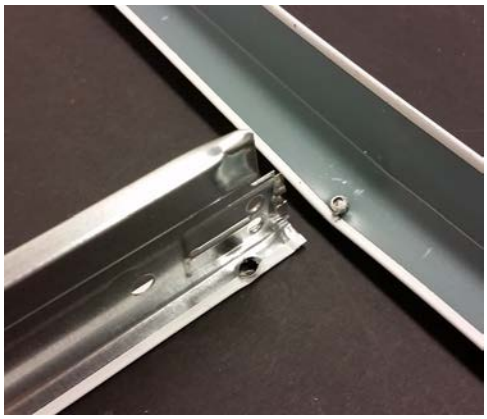

b) Typical failure mode (USG2015-Sp10 is shown)

Figure 4: Typical test result and failure mode.

3 SHAKING TABLE TESTING

A shaking table test was conducted in a 6.1 m by 6.1 m (20 ft by 20 ft) test frame specially designed and built at the University of California, Berkeley for testing suspended ceiling systems [3].

3.1 Test Frame and Test Time History

The test frame [3] enables the installation of suspended ceiling systems at an elevated position in order to be tested via shaking table tests. The shaking table was controlled by a test time history which was developed earlier [4] by following the requirements of ICC-ES AC156 [5]. This time history accounts for the amplification of the seismic demand over the elevation of buildings. To avoid any additional amplifications, the test frame is designed to be very stiff with frequencies greater than 20 Hz in all three principal axes. The frame is bolted to the top of the shaking table. Figure 5a shows the major components of the test frame. A typical view of the suspended ceiling installed into the frame is presented in Figure 5b.

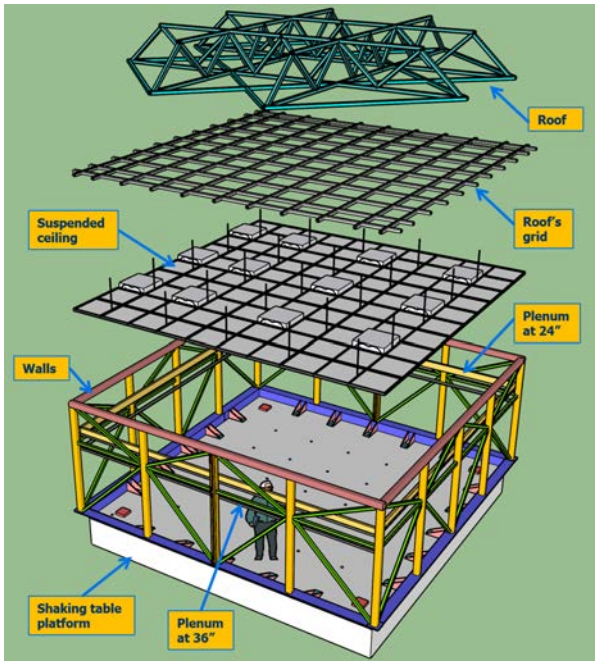

a) Major components

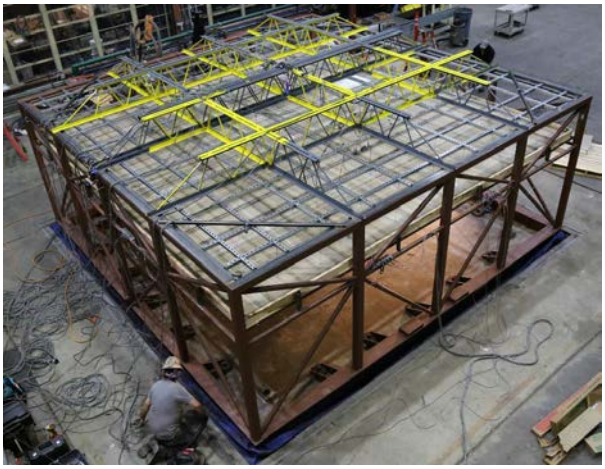

b) Typical view with ceiling installed

Figure 5: 6.1 m by 6.1 m test frame for testing suspended ceiling systems.

Prior to the time history testing a resonance search was conducted by imposing a white noise signal to the suspended ceiling system via the shaking table. The time history testing procedure was based on a value of spectral acceleration at short periods, S_S [6], which controls the level of shaking [5]. The first time history test was conducted at $S_S = 2.0$ g, which was incrementally increased by 0.25g for the following tests up to $S_S = 2.75$ g.

3.2 Suspended Ceiling System Tested

The suspended ceiling tested via the shaking table tests is summarized in Table 2.

Description	Characteristics or value
USG system identifier (duty rating)	USG DXT26 (heavy)
Main tee (USG ID)	DXT26
Cross tee (USG ID)	DXT 424, DXT 222
Wall molding (USG ID)	M7
Panels (USG ID)	GLIP 3260 (two layers)
System weight (including grid weight), kg/m^2 (lb/ft^2)	19.5 (4.0)
Perimeter wires	Yes (all 4 sides)
Stabilizer bars	None
2 adjacent floating sides	ACM7 Clip
2 adjacent fixed sides - tight no gap	Pop rivet
Floating wall clearance, mm (in)	19.1 (3/4)
Compression post	At 1.83 m (6 ft) from floating sides

Table 2: Suspended ceiling system tested via shaking table tests.

3.3 Instrumentation

The suspended ceiling, the test frame, and the shaking table were extensively instrumented. In addition to position transducers and accelerometers commonly used for testing suspended ceiling systems, a few strain gages were installed at critical locations. This extensive instrumentation was aimed at a detailed analysis of the performance of critical components. Figure 6a shows the schematic of the instrumentation. In this image "A" stands for accelerometer, "DA" stands for position transducers measuring displacement at the perimeter, "DR" stands for position transducers measuring displacement across the joints, "S" stands for uniaxial strain gages, and "R" stands for tri-axial strain gages. Typical instrumentation around the main tee's joint is presented in Figure 6b.

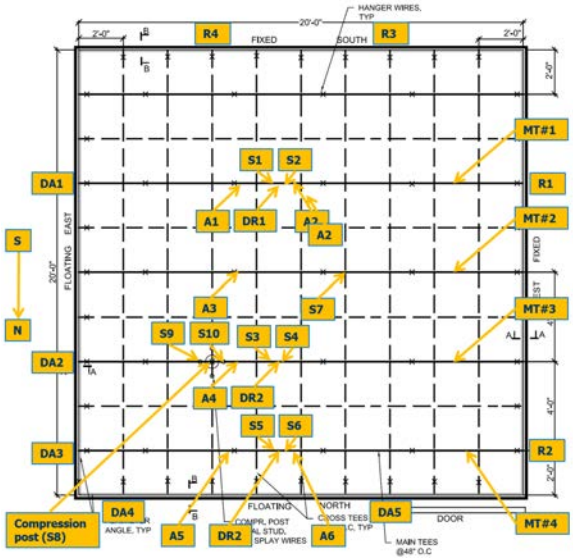

a) Schematic of instrumentation

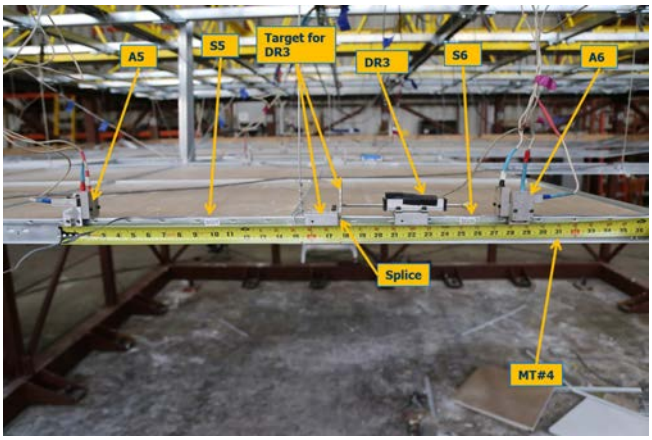

b) Example of main tee joint (splice) instrumented with position transducers, strain gages, and accelerometers

Figure 6: Instrumentation.

3.4 Shaking Test Results: Overall Performance

The spectral accelerations generated from the accelerations recorded on top of the shaking table enveloped the required response spectra specified by the AC156 document [5]. Typical

results are presented in Figure 7 for S_S = 2.25 g. As presented in these images, the spectral plots enveloped the required response spectra shown by the red dashed line.

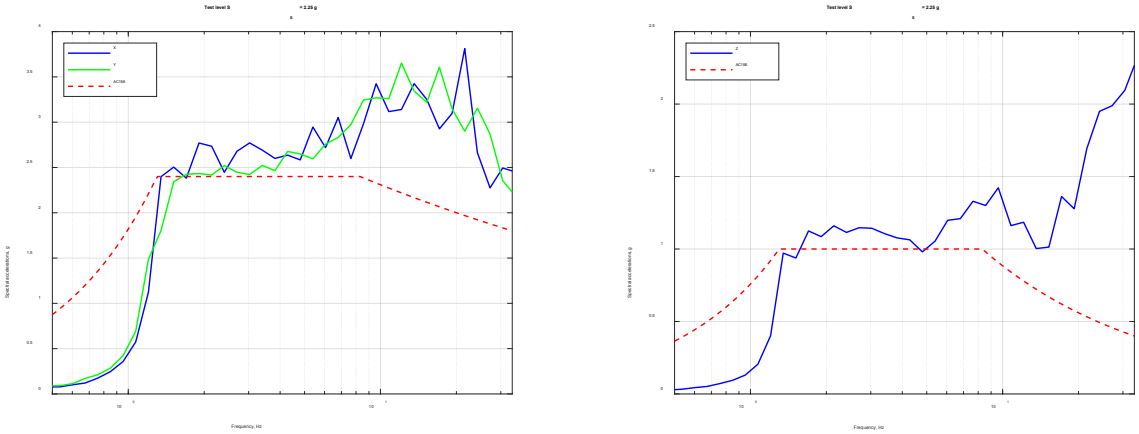

a) Spectral accelerations in X&Y axes b) Spectral accelerations in Z axis

Figure 7: Typical spectral plots (S_S = 2.25 g is shown).

Overall performance of the system is summarized in Table 3.

S_S, g	Description of anomaly or failure if any
2.0	No failure of the system was observed
2.25	No failure of the system was observed
2.5	Six 0.6 m x 0.6 m (2 ft x2 ft) panels dropped; integrity of the grid somewhat compromised
2.75	Cross tees disengaged from the wall angles with less than 50% of the tiles dropped

Table 3: Overall performance of the system in the shaking table tests

4 NUMERICAL MODELING AND ANALYSIS

A suspended ceiling system is a complex structure consisting of many components and joints and it performs in a nonlinear manner. To make it realistic, a number of components must be modeled as nonlinear elements with some of the representative examples listed below. First, each panel is free to slide within the grid and when the gap between the grid and the panel is closed, the panels engage in a stiff planar system producing a diaphragm stiffness in the horizontal plane. As a result, the fully engaged grid-panel system prevents distortion of the grid. Second, all hanger wires can develop restraining forces only in tension and they have low stiffness in compression. Hence, the hanger wires need to be modeled as nonlinear tension-only members. Third, the components on both the floating and fixed sides perform in different ways depending on tension or compression. The connections on the fixed side have much larger stiffness in compression than that in tension. In addition, the connection on the fixed side can yield at high levels of seismic excitation. Fourth, the travel of the system on the floating side can exceed a gap (typically 19 mm or ¾ in) and as such, these elements have to be modeled as nonlinear gap elements.

It is always a challenge to incorporate all these nonlinearity effects into a finite element model. A few attempts at developing a finite element model of a suspended ceiling system were conducted earlier (see [7,8], as representative examples).

4.1 Grid modeling

The main tees, cross tees, and the compression post were modeled by elastic frames (in SAP2000 [9] terminology). The hanger and splay wires were modeled as nonlinear links that work in tension only. The stiffness of the wire was estimated based on its cross section and the material properties of mild steel. A view of the grid modeled in SAP2000 is presented in Figure 8. The main tees are presented in blue and the cross tees are shown in red. The system consists of five main tees and the rest of the system is assembled from cross tees. A model of the compression post with splay wires and cross-sections of the main grid components are presented in Figure 9.

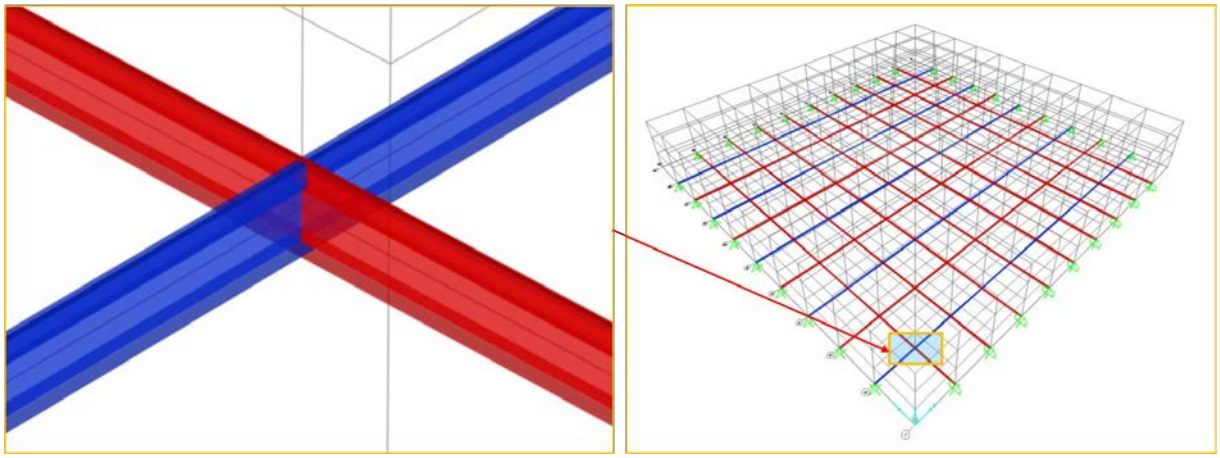

Figure 8: Grid model: overall view on the right and closeup view of MT to CT connection on the left.

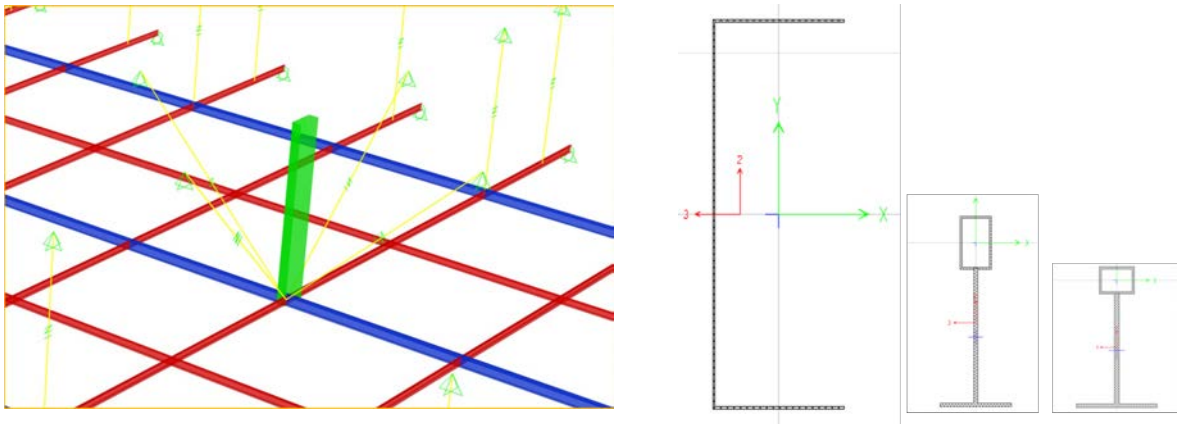

a) Compression post modeling b) Cross sections of post, MT, and CT

Figure 9: Details of grid model.

4.2 Modeling panels

The 0.6 m by 0.6 m (24 in by 24 in) panels were modeled as rigid elements with the weight of the panel lumped at its middle. Based on the tolerances of the grid and the panel, the clearance between the panel and the grid is 2.74 mm (0.108 in) on each side. To model this clearance, gap elements were introduced at each corner of the panel as presented in Figure 10. The accumulated weight of the panels and the grid is equal to 19.5 kg/m^2 (4 psf) distributed weight multiplied by the area of the system (37. 21 m^2 or 400 ft^2). The gaps in both horizontal directions are 2.74 mm (0.108 in), whereas the gap in the vertical direction is equal to zero.

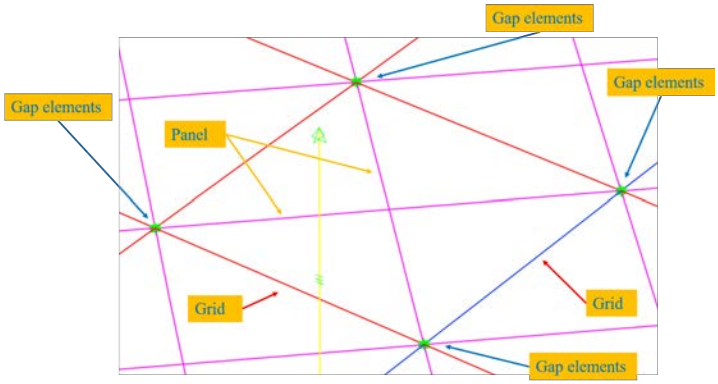

Figure 10: Details of panel modeling.

4.3 Modeling of perimeter connections

Figure 4a shows a typical performance of a perimeter connection that displays two major performance behaviors. First, the performance of the connection is direction dependent. The stiffness of the connection in the direction toward the wall (compression that corresponds to the negative force and displacement in the plot) is much higher than that in the opposite direction (tension). Second, the connection can undergo plastic deformation in tension.

This performance was modeled by combining two nonlinear links (SAP2000 terminology). The first link was a gap element and the second was a nonlinear link with the Wen plastic model as presented in Figure 11.

The floating side is modeled by friction elements in the papers reviewed earlier. This model does not reflect the actual performance of the system because the hanger wires work as a set of pendulum systems that result in lifting the grid on the floating side. Therefore, the effect of friction on the floating side is most likely negligible. Therefore, the floating side connections were modeled as frictionless sliders.

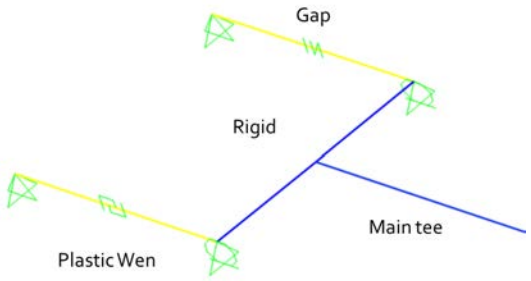

Figure 11: Details of perimeter connection modeling: fixed side.

4.4 Overall performance of the model

Based on the experimental data and observations during the shaking table tests, the failures usually occur at the cross tee connection when a tension force exceeding its capacity is applied. Although the tension capacity of the main tee is greater than that of the cross tee, it can also be a location for failure. Therefore, the main critical parameter to monitor during finite element analysis is the tension axial force in the tees. Typical results for one of the tees are presented in Figure 12.

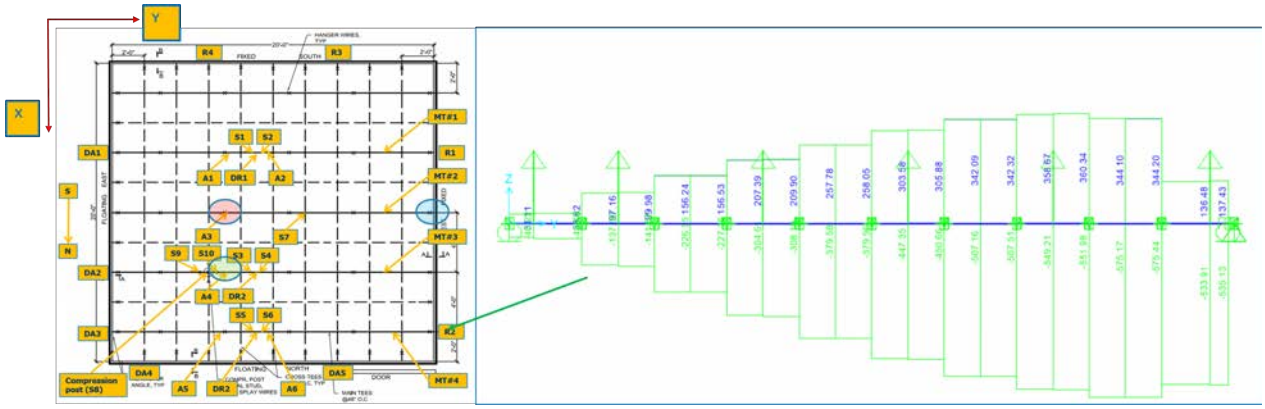

Figure 12: Results of FEA: tension forces in tees.

The same analysis can be done from tee to tee, but it can be less obvious where the tension forces are experiencing a maximum. To make the process of analyzing the numerical results more efficient, a special code was developed in the Matlab environment [10], that shows all tension forces in all cross tees. Figure 13 shows the result in 3D and Figure 14 shows the same result in the plane. In the latter plot, the color of the dot at the middle of each frame depends on the value of the tension force.

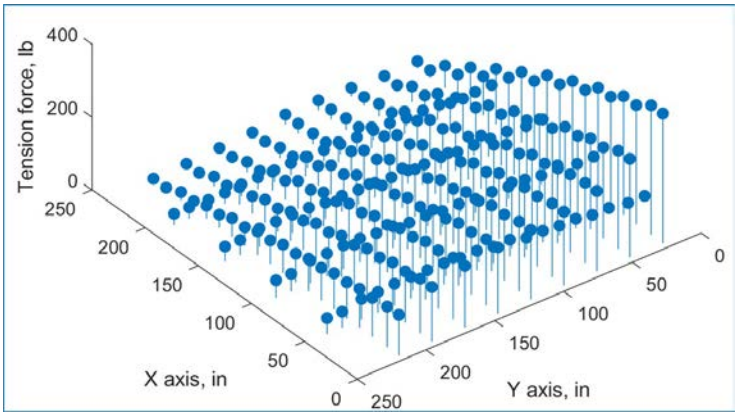

Figure 13: Maximum axial tension forces in cross tees (3D).

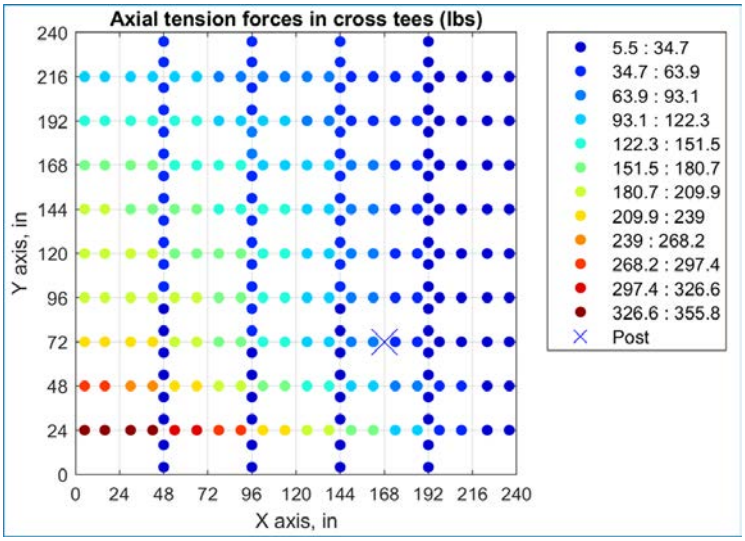

Figure 14: Maximum axial tension forces in cross tees.

5 CONCLUSIONS

Based on the extensive component test data a finite element model of the USG system was developed. The model closely replicate the system failures observed during the shaking table tests. The developed model will be used for the following optimization studies of the ceiling's performance: (1) the effect of the post's location or the removal of the post; (2) the effect of having an additional screw through the wall molding; (3) the optimization of light fixture locations; (4) the effect of a plenum depth; (5) the correlation seismic performances in 20'x20' test frame to that in large partitions; (6) the effect of seismic joints in large partitions and many others. The numerical modeling will help find solutions for future product development and performance simulations of suspended ceilings at larger scales.

ACKNOWLEDGMENTS

Special thanks are due to the USG Corporation for funding the project. The authors would like to acknowledge Ms. Holly Halligan of UC Berkeley for editing the paper. A part of numerical modeling was conducted by Sensor Fusion and Monitoring Technologies, LLC.

REFERENCES

[1] Shakhzod M. Takhirov. Evaluation of Wall Connections of USG Suspended Ceiling's Grid in Monotonic and Cyclic Testing. Report No. CEE-SL-STI/2015-01. Department of Civil and Environmental Engineering, University of California, Berkeley, July 2015.

[2] Shakhzod M. Takhirov and Amir Gilani. Component Tests of USG's Wall Perimeter Connections and Joints. Structures Laboratory Report 2021/02, Department of Civil and Environmental Engineering, University of California, Berkeley, April 2021.

[3] Shakhzod M. Takhirov and Amir Gilani. Development of 20' by 20' Test Frame for Experimental Seismic Evaluation of Large Suspended Ceiling Systems on Shaking Table: Design and Dynamic Analysis. Structures Laboratory Report 2018/01, Department of Civil and Environmental Engineering, University of California, Berkeley, January 2018.

[4] Amir Gilani and Shakhzod Takhirov. Current U.S. practice of seismic qualification of suspended ceilings by means of shake table tests, INGEGNERIA SISMICA journal, Italy: Vol. XXVIII, No. 1, pp. 26-42, 2011.

[5] International Code Council Evaluation Service Inc. (ICC-ES). Acceptance Criteria for Seismic Qualification by Shake-Table Testing of Nonstructural Components and Systems, AC156, ICC-ES, 2015.

[6] American Society of Civil Engineers, ASCE. Minimum Design Loads and Associated Criteria for Buildings and Other Structures (ASCE7-16). 800 pp. 2 volume set. 2017.

[7] Arash E. Zaghi, Siavash Soroushian, Alicia Echevarria Heiser, Manos Maragakis and Amvrossios Bagtzoglou (2016). Development and Validation of a Numerical Model for Suspended-Ceiling Systems with Acoustic Tiles, Journal of Architectural Engineering, 2016, Vol. 22, No3, pp. 04016008-04016008-13, DOI: 10.1061/(ASCE)AE.1943-5568.0000213.

[8] A. A. Echevarria, A. E. Zaghi, S. Soroushian and E. M. Maragakis (2012). Seismic Fragility of Suspended Ceiling Systems. Proceedings of 15th World Conference on Earthquake Engineering, September 24-28 2012, Lisbon, Portugal.

[9] SAP2000 (2011). Computers and Structures, Inc.

[10] MathWorks. Matlab Version R2020a. 2020.